Using Strain Energy Method to Estimate Buckling in Steel Column AISI 1312 during Effects of Fire Hazard

Article *in* Key Engineering Materials · June 2022

DOI: 10.4028/p-iz1y6z

CITATIONS
0

READS
5

2 authors:

Ali Hussein Fahem
Al-Furat Al-Awsat Technical University
12 PUBLICATIONS **14** CITATIONS
SEE PROFILE

Malik N. Hawas
Al-Furat Al-Awsat Technical University
41 PUBLICATIONS **36** CITATIONS
SEE PROFILE

Key Engineering Materials
ISSN: 1662-9795, Vol. 924, pp 3-16
doi:10.4028/p-iz1y6z

Submitted: 2022-01-31
Revised: 2022-03-28
Accepted: 2022-03-28
Online: 2022-06-30

Using Strain Energy Method to Estimate Buckling in Steel Column AISI 1312 During Effects of Fire Hazard

Ali Hussein Fahem[1,a*], Malik N. Hawas[1,b]

[1]Al-Furat Al-Awsat Technical University, Iraq

[a*]ali.h.fahem@atu.edu.iq, [b]com.mlk@atu.edu.iq

Keywords: Strain Energy, Buckling, Creep, steel AISI 1312, Fire Hazard

Abstract. A Group of three specimens from 1312 steel were subjected to range of elevated temperatures (700, 800, 900) Celsius to demonstrate the hazard of fire on steel columns mechanical proprieties. The results show a dangerous increase in creep strain buckling after 60 minutes from the beginning of the test and after 67 minutes failed to occur. Mechanical tests for normal and elevated temperatures were made to compare the fire hazards, the results depict reduction by 29%, 46%, 55% for young modulus of elasticity for elevated steel specimens (700, 800, 900) °C. for yield strength the value decreased by (128.4, 169.6, 189) Mpa for specimens (700, 800, 900) °C respectively. The ultimate stress reduction by (64, 78, 83) % from the normal value. whenever higher temperatures go up the lower the ultimate strain falls dawn by (50, 60, 66) % to the original ultimate strain value 0.5. the 0.2 strain % is decreased from 0.0029 to 0.0027 for 700 °C and increased to 0.011, 0.015 for (800, 900) °C respectively.

1. Introduction

To attain weight loss and decrease the production fee of metal carrying structures, engineers frequently design steel columns with uniform move sections with multi-phase carriers. Since columns are normally compressed by payload, self-weight, and so on., the principal element in the usage of such vectors is their flexible stability. This paper considers the elastic balance of a three-section phase column difficulty to centralized compressive forces. The trouble of flexible stability of multi-level columns is satisfactory analyzed the use of automatic structural analysis techniques. This is a try and develops an analytical version for computing flexible buckling essential hundreds suitable for constructing software program applications. The foundation for constructing analytical model of the stepped column sensitive buckling load is the famous Euler version [1-3].

Determining the important buckling load of a column with uneven go-phase can be a complicated mission primarily based on different load and boundary situations. An extra unique approach to the research of buckling of unequal columns with spring guide under combined unmarried and line loads is offered in [4]. The paintings [5] units the crucial differential equation for the buckling of multi-degree, unequal beams beneath more than one concentric not unusual force. Some authors have cited instances of axially compressed uneven columns subjected to stepped axial loads that act eccentrically on columns [6,7]. In [7], the impact of preliminary mistakes on the stability of uneven metal additives under eccentrically applied axial hundreds became additionally considered. In a few publications, expressions are used to describe the distribution of uneven column bending inertia and the distribution of axial forces appearing on the column [8,9]. The effects of the proposed strategies are frequently compared with the effects of the finite detail technique (FEM) [10]. In addition, a few authors have pointed to using the idea of powerful lengths [11]. Given the complexity of the trouble, lots of attempt has been made to expand a model improvement method useful for quick however fairly correct calculations of the essential buckling load of conical help [12,13]. On the opposite hand, some authors have executed a balance evaluation of non-prismatic columns primarily according to modified vibration modes [14]. In addition, some authors have investigated the stableness of composite columns and beams with variable move sections [15-16]. In popular, the elastic balance hassle of a stepped column can be solved in several ways, however, most of the research to date may be broken down into two foremost processes.

Concrete-crammed steel tubular participants (CFST) had been broadly used inside the creative industry because of their excess electricity, brilliant flexibility, and earthquake-resistance [1–3]. Yet, conventional CFST factors utilized in tall homes and lengthy-time period bridges are much less durable because of corrosion problems, ensuing in higher renovation expenses. With the benefits of excessive corrosion resistance, aesthetic appearance, and fireplace resistance, chrome steel can lessen preservation fees due to the fact the factors may be uncovered immediately to the environment with no protective coating. Thus, the opportunity layout of Stainless-Steel Tubular Elements (CFSST) filled with concrete is seen as a promising answer, with the blessings of the CFST device and the high corrosion resistance of chrome steel. Although CFSST and CFST systems depend on the influence of stress, the conversion of CFSST individuals from conventional carbon metallic to CFST stainless steel outcomes in notably exceptional strengths due to variations of their cloth houses. CFSST individuals ought to not be designed with it. One set of equivalents same as CFST individuals.

Numerous researches on CFST individuals [4–10] have systematically investigated the neighborhood and well-known buckling power of the device and advised corresponding design methods. In evaluation, the survey of CFSST individuals has most effective just began. Han et al. [11] examined current works on the performances of CFSST participants and mentioned future studies guidelines for the CFSST device. There was [12] an experimental performance of CFSST columns below compression and located that current strategies for calculating CFST participants have been too conservative while applying it to CFSST. Young and Ellobody [13] tested concrete-crammed bloodless-formed chrome steel pipe columns beneath axial compression and suggested layout tips for cold-fashioned CFSST columns. In addition, there were many checks of reinforced and unreinforced CFSST columns beneath compression indicating the bolstered contributors furnished more limitation of the concrete core than the unreinforced contributors [14]. CFSST brief columns underneath axial compression was studied and proposed a design method primarily based on present-day CFST design rules [15], [16] and. [17]. Different CFSST participant structural constituents, namely joint slip, flex, and hearth resistance behavior, are Chen et al. It becomes investigated. [18,19] and Ellobody [20].

Buckling seems to be a primary form of failure in metal columns which are subject to axial hundreds. Because it's far underneath stress that's much less than the very last compressive strain of the material. Bending depends on the elasticity modulus decreasing with growing temperature [1], and consequently presents a certain difficulty at expanded temperatures, as an instance, fires in nuclear power vegetation and in extreme accidents. Crawling is likewise a major issue for structural integrity and the pipe ruptures at high temperatures because of the the crawling rate increases with growing temperature at a pressure [2]. In unique, throughout creep tests, it became cited that the breaking time of metallic columns under axial compression is less than the axial pressure [3]. Steel is one of the maximums as common metals and is used for a spread of industrial functions, inclusive of constructing substances and pipes. As such, many previous studies have examined the process of buckling and creep buckling in a spread of applications and in distinctive demanding conditions. The disorder of Type-304 chrome steel bars was calculated under cyclic loading at temperatures of 300 and 560 ° C [4]. In addition, [5] buckling tests was carried out at 470–550 C. In addition, [6] analytical techniques are suggested to predict fire resistance underneath a constancy of external hundreds and models used experimental findings according with the usual approach for “American structural metal ASTM-A36. Ng”. A numerical simulation of stainless-steel structural columns was used to check the influence of different factors, along with geometric flaws and residual strain at crucial temperatures [7]. The impact of the preliminary geometric flaws on the buckling performance of skinny cylindrical tube columns beneath the outer pressures was tested [8]. According to Joe et al. [9], “the buckling load of the stainless-steel plate under axial compression and a wide range of room temperature between 1200 ºC". The steel column buckling resistance of at room temperature is appropriately identified and, at high temperatures, it isn't completely mounted because of a loss of sufficient experimental facts. To our know-how, there are some empirical statistics on creep buckling at temperatures above six hundred ºC.

In this have a look, the creep buckling breakage time of 1213 sheet metal columns became measured under axial compression. Crepe tests have been accomplished under 3 diverse temperature

circumstances: seven hundred, 800, and 900 ° C to show the influence of temperature on plate buckling. The relationship between fracture time fall and compressive pressure was determined by the using different pressures related to the buckling pressure described with the aid of et al. [9]. We investigated the axial and historical past of the mechanical conduct of the plate column at some point of the creep test and advanced an experimental system for predicting the break time of stainless-steel sheets by the use of the LMP model. Another experimental formula that could be used as an alternative to the traditional experimental correlation turned into according to the plate column deviation background from the images taking from the experiment.
This work is experimental and uses a numerical simulation on restrained 1312 steel H-section columns under axial compression whose reaction and failure are exposed to fire. There was a steady-state tensile tests of the high-temperature mechanics of S30408 (EN1.4301) 1312 steel. The reduction of strength factors, elastic modulus and stress strain curves under various temperatures appeared. Secondly, in accordance with the ISO-834 standard fire curve, we performed axial compression tests in fire on columns with axial restraint.

2. Methodology

Features of Materials at Multiplied Temperatures

Information on the behavior of substances at expanded temperatures resolves each Fourier warmth switch equations and structural modeling. consequently, it is handy for dividing this bankruptcy into separate sections for the two phases of evaluation. lots of this bankruptcy will cognizance on steel, structural, and each rebar and urban. Two RILEM reviews (Anderberg, 1983; Schneider, 1986a) published good sized amounts of statistics on both materials. reviews are a compilation of contemporary statistics collected on a one-off foundation using aselection of trying out techniques that are not presently standardized. Further, statistics is provided for timber, masonry, and aluminum, despite the fact that wood data is much less required as contemporary design techniques generally do no longer require temperature-based belongings information. For masonry, such statistics isn't always required in any of the exact layout strategies presently in use.

2.1 Thermal Data

The Fourier equation of warmth transfer is:

$$\nabla(a(\Delta\theta)) = \dot{\theta} \tag{1}$$

Wherein, θ is the distance-based temperature and a stands for the temperature dependent thermal diffusivity to be in relation to the the density ρ. We also have thermal conductivity λ and the particular heat c_r

$$a = \frac{\lambda}{\rho c_v} \tag{2}$$

The data for the calculation of the thermal reaction is typically most effective required for concrete, steel and aluminum. Yet, masonry thermal response calculations can be executed, they're typically now not important. electricity measurements for timber are executed on cores, which can be considered unaffected with the aid of temperature or have a tolerance to the effect of temperature by an application of something to the allowable stresses at the thickness of the article. consequently, thermal statistics is in general now not essential, even though in some instances in which the temperature upward push in a middle is probable to be big, expertise of thermal diffusivity is required. The statistics for the calculation of the thermal response is typically handiest required for concrete, metal, and aluminum. even though masonry thermal response calculations may be done, they're normally now not necessary. Energy calculations for wooden are finished on cores, unaffected with the help from the temperature, and have a tolerance to the effect of temperature by an element applied to the reasonable stresses according to thickness. Therefore, thermal information is normally not necessary. However, in a few cases wherein the temperature rise in a middle is in all likelihood to be big, there is a requirement of knowledge of thermal diffusivity.

2.2 Steel

The feature values concerned are sensibly free from steel use (structural or reinforcing) and its strength or grade.

2.3 Density

The steel density is used because its ambient is 7850 kg/m³ over the usually experienced temperatures.

2.4 Specific heat

According to Malhotra (1982a), the steel specific heat of c_a(J/kg°C) is:

$$c_a = 475 + 6{,}01 \times 10^{-4}\theta_a^2 + 9{,}64 \times 10^{-2}\theta_a^2 \quad (3)$$

Equation (3) and test data from Pettersson et al. (1976) and Stirland (1980) are a version of Malhotra (1982a) as in Fig. (1). The discontinuity in this heat is at around 750°C, Equation (3) only is up to this value. EN 1994-1-2
is equations up to 1200°C :
For

"$20°C \leq \theta_a \leq 600°C$

$$c_x = 425 + 0{,}773\theta_a - 1{,}69 \times 10^{-3}\theta_a^2 + 2{,}22 \times 10^{-6}\theta_a^3" \quad (4)$$

"For $600°C \leq \theta_a \leq 735°C$:

$$c_x = 666 - \frac{1302}{\theta_a - 738} \quad (5)$$

For $735°C \leq \theta_a \leq 900°C$: "

$$c_a = 545 + \frac{17820}{\theta_a - 731} \quad (6)$$

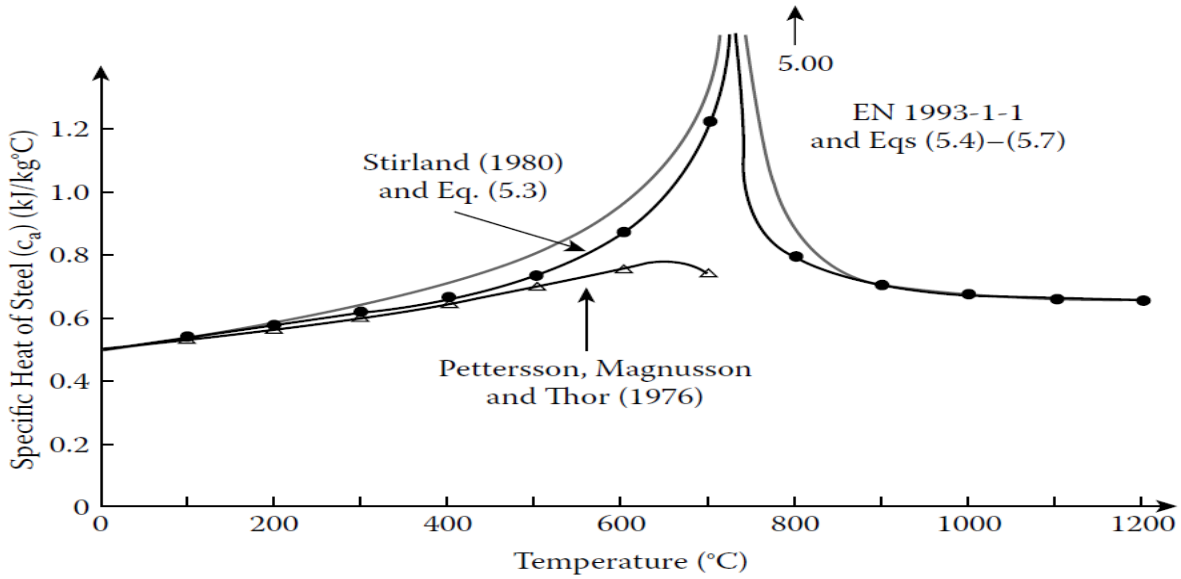

Fig. (1) Specific heat Variation of steel with temperature.

For $900 \leq \theta_a \leq 1200°C$:
$c_a = 650$

2.5 Thermal conductivity

For $20°C \leq \theta_a \leq 800°C$:

$$\lambda_a = 54 - 33{,}3 \times 10^{-3}\theta_a \quad (7)$$

For $\theta_a \geq 800°C$:
$\lambda_a = 27{,}3$

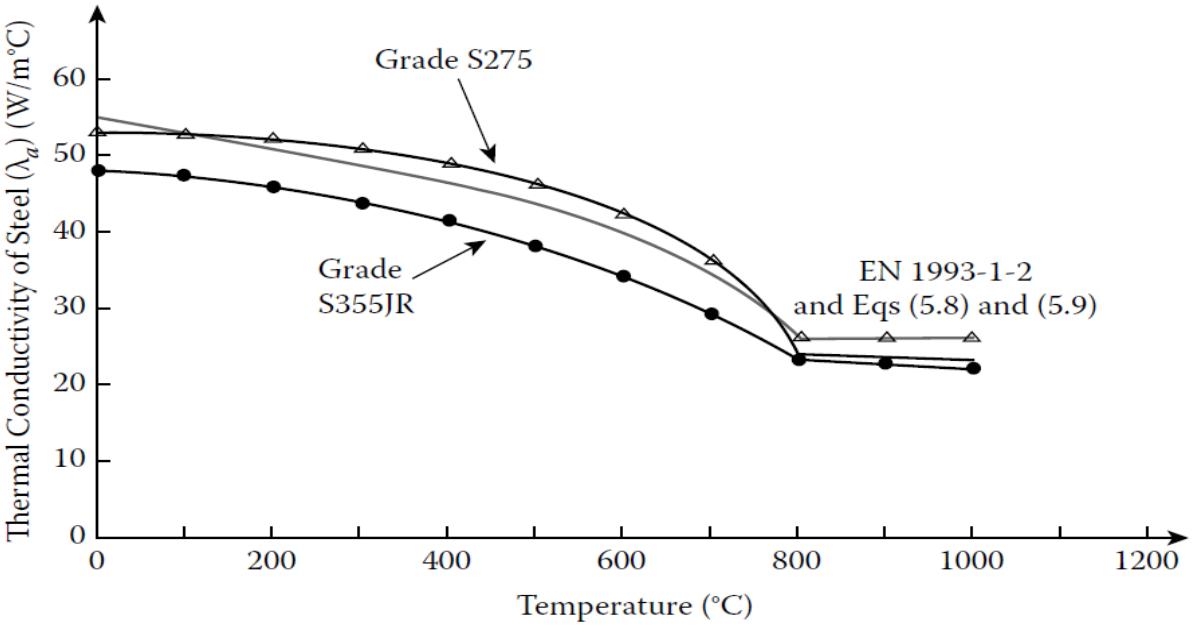

Fig. (2) A variety of thermal conductivity of steel with temperature.

2.6 Thermal diffusivity

The data given of the density, the thermal diffusivity, specific heat and the standard density values of steel (m2/hr.) show a "sensibly linear relationship with temperature up to 750°C based on:

$$a_a = 0{,}87 - 0{,}84 \times 10^{-3}\theta_a" \quad (8)$$

2.7 Materials Data

To be able to decide the structural reaction within the occasion of a fireplace, it is essential to expand a constitutional law concerning the mechanical conduct of the relevant fabric at high temperatures. The entire system is vital handiest whilst entire evaluation is performed to calculate the error and displacement. in case handiest want to calculate the weight potential, a more restrained dataset is available. In reality, an awful lot of the preliminary research to evaluate material behavior become geared toward determining particular houses, including the tensile strength of metal and the compressive power of concrete at excessive temperatures. It was no longer long before the need for a constitutional version became recognized. the standard test technique has been developed via corporations with reference to ambient situations which includes British standards. but, even as the Comité Européende Normalization (CEN) is thinking about proposals for such requirements, no such trendy is legitimate for checking out at high temperatures. because crawling (or resting) may be very excessive at excessive temperatures, the weight (stress) or price of pressure used within the high-temperature take a look at performs a far greater critical position than the ambient conditions. The heating charge used to situation the sample also impacts the very last test results.

2.8 Checking out Régimes

Most of the early experimental investigations used stationary test approaches wherein a pattern become heated at most of the early experimental investigations used desk bound test processes wherein a pattern became heated at a steady fee of temperature upward push in an oven and conditioned through immersing it for a specific time at the test temperature to be a consistent temperature. The phase earlier than loading to determine the desired belongings. The assessment of the strength became generally done with a consistent anxiety load price, either in tensile assessments on metal or compression checks on concrete. The problem of using a steady pressure ratio is a complete stress-stress curve is not possible for concrete. However, when the take a look at is performed at a steady fee of deformation, the ensuing hundreds may be calculated and the whole strain-strain curve could be achieved, when the test bench is satisfactorily rigid. Traditional creep checks are accomplished by using loading a heated sample with a consistent load and calculating the ensuing elongations over an appropriate time period.

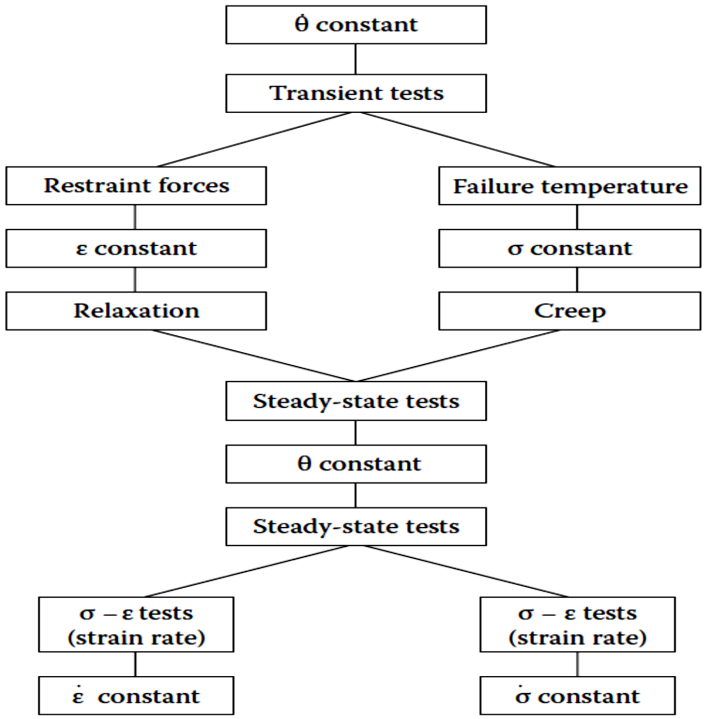

Fig. (3) Testing régimes for the determination of mechanical performances of materials at higher temperatures.

2.9 Unrestrained thermal expansion

For $20°C \leq \theta_s \leq 750°C$:

$$\varepsilon_x(\theta_x) = -2{,}416 \times 10^{-4} + 1{,}2 \times 10^{-5}\theta_x + 0{,}4 \times 10^{-8}\theta_x^2 \quad (9)$$

"For $750°C \leq \theta_s \leq 860°C$":

$$"\varepsilon_2(\theta_x) = 11 \times 10^{-3}" \quad (10)$$

"For $860°C \leq \theta_s \leq 1200°C$":

$$"\varepsilon_x(\theta_x) = -6{,}2 \times 10^{-4} + 10^{-5}\theta_x + 0{,}4 \times 10^{-8}\theta_x^{2"} \quad (11)$$

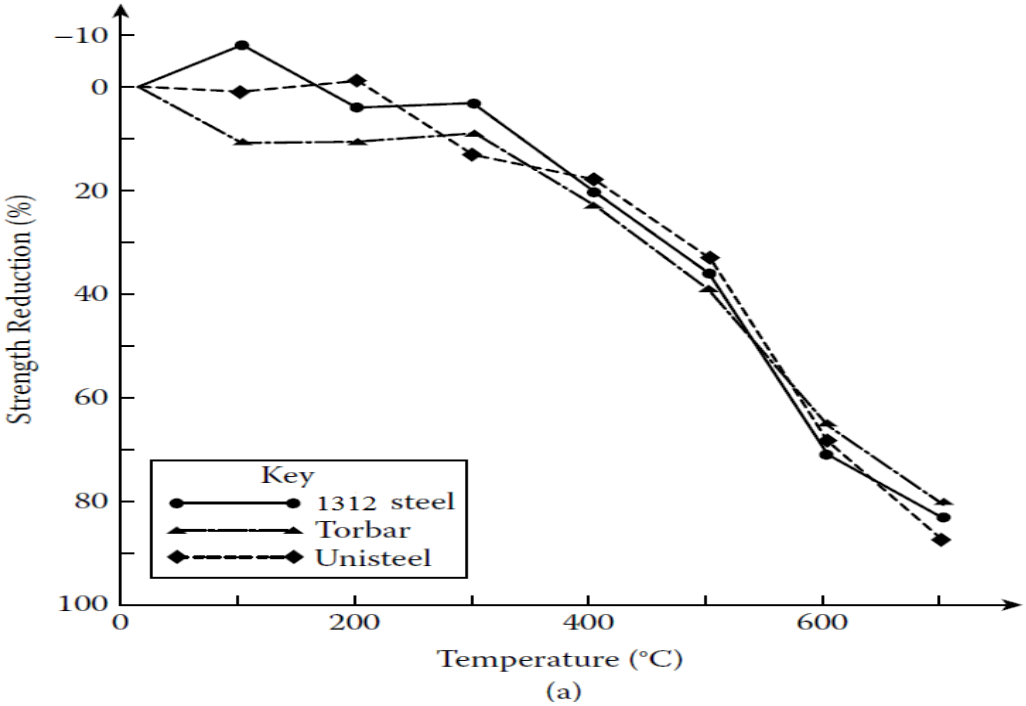

Fig. (4) Variation of normalized strength of reinforcing steels with temperature.

2.10 Creep

In the case of steel, isothermal creep (i.e., creep calculated at constant stress and constant temperature) turns to be more substantial than ~ 450 °C if reinforcement and structural steels obtain their maximum load capacity. General data on the creeps of steels is in Fig. (5) (Enderberg, 1988). It is a common in the analysis of the creep data using a time-point approach to compensating for the mandrel's temperature with the secondary creep.

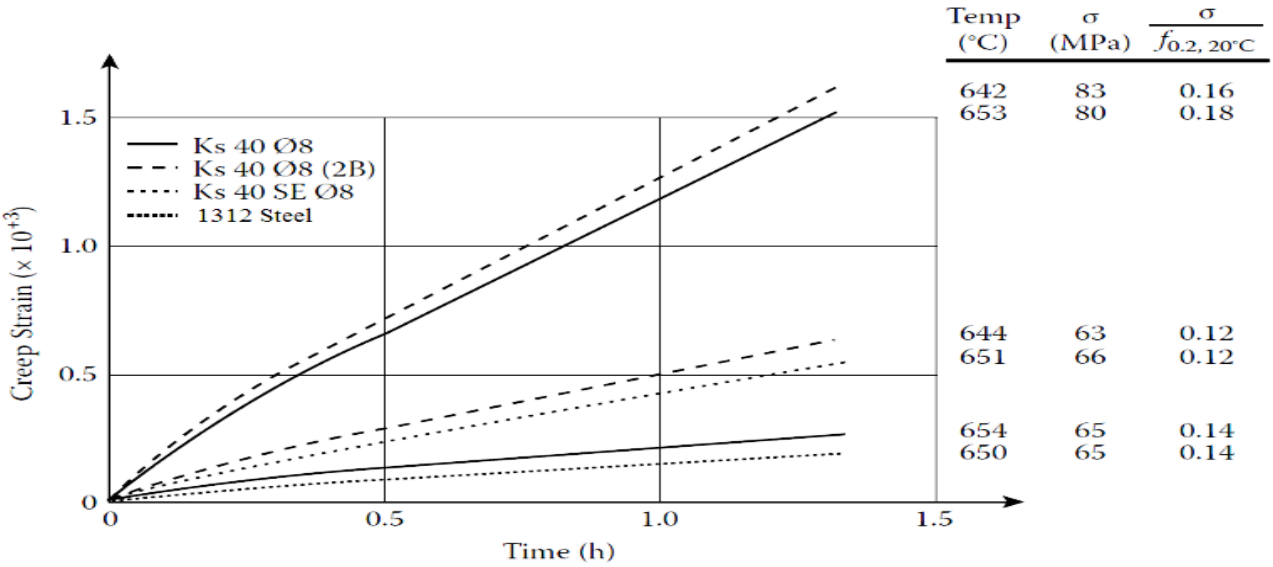

Fig. (5) Creep strains for reinforcing steels at elevated temperature.

2.11 Calculation Approach

Examinations of fire resistance of systems is a complex manner as it includes different aspects such as the growth and length of the fire, the temperature distribution in structural factors, structural aspect interactions, modifications in cloth houses, and effects on structural machine masses. The system typically entails 3 separate additives: (1) fire risk evaluation to pick out hearth scenarios and show the influence of every situation on adjoining structural participants; (2) thermal evaluation to calculate the temperature records in every detail, and (3) structural evaluation to decide the forces and stresses in each element and the nearby or innovative collapse of the structure in any fireplace threat situation. the primary motive of such evaluation is to determine the time at which a shape is capable of withstand failure whilst uncovered to hearth, electricity at a predetermined time, or time to attain a specific electricity discount. fuel resulting from an herbal fireplace or a widespread oven check to attain a positive temperature while a structure or structural member is uncovered to temperature. The integrity of an issue, that is, the capacity to withstand flame passage thru gaps inside the structure, isn't always commonly calculated; that is best decided the usage of widespread oven testing, as this sort of failure commonly applies to materials inclusive of fireplace doors and other remaining structures. therefore, the last kingdom of integrity can't be considered in addition inside the calculation.

3. Results and Discussion

Fig. 7 shows an ordinary axial displacement of the check column at some stage in the experiment of creep buckling at 900 ºC. The test column to start with multiplied is because temperature grows, and the axial displacement extended with time at the most axial shift, showing that the plate column temperature achieved the optimal cost, the axial compressive strain turned into implemented to the column. The in-aircraft shift then commenced for decreasing because of creep buckling. Fig. 7 shows that it turned into determined that the axial displacement progressively accelerated following the strain loading. but, the trade within the displacement improved swiftly after 40 min of making use of the load, that's because of the onset of plastic buckling of the column .Then, the column subsequently distorted, showing an unexpected lower inside the axial displacement (i.e., nearly countless exchange

within the axial displacement. (discern eight shows the lateral deflection in opposition to the time curve for the identical temperature and cargo situations for that displacement curve as Fig. 7 shows. The curve in Fig. 8 is captured photos of the take a look at column at some point of the creep buckling test. It is easy to process the images, proven in Fig. 6, and accomplished the IMAGEJ freeware. The images can give the plots of intensity along the centerline inside the horizontal direction as in Fig. 9. When thickness of the examined columns became 2. zero mm, the length in a unit pixel was based on an earlier image of the take a look at. The calculations of the lateral deflection are conducted by counting the horizontally moved pixels, and the lateral deflection curve final plot as a feature of time. The curves were acquired, except in the two cases where the photograph records are missed because of the high-velocity diagram software malfunction. The calibration shifted to decide the period to keep with unit pixel carried out for every test. The lateral deflection in opposition the time curve in Fig. 8 resembles overall strain curve in opposition to time in creep test under tensile pressure". When the stress in opposition to time curve, the primary and tertiary creep reduces than the secondary creep stage where the take a look at column was laterally deflected at a constant fee. Yet, the price, the deflection price reputedly commenced for increasing about forty mi corresponding to the plastic buckling onset in the curve in Fig. 7. Thus, the lateral deflection charge multiplied to about infinity, that results in the eventual crumble of the column. This confirms [3] and [5] findings of metallic column and an aluminum alloy. The deflection fee is for an H-phase steel column. Both the in- and out-of-plane shifts of an aluminum-alloy plate column are confirmed. They stated that there is a negative correlation between lateral deflection price within the 2d degree with strain.

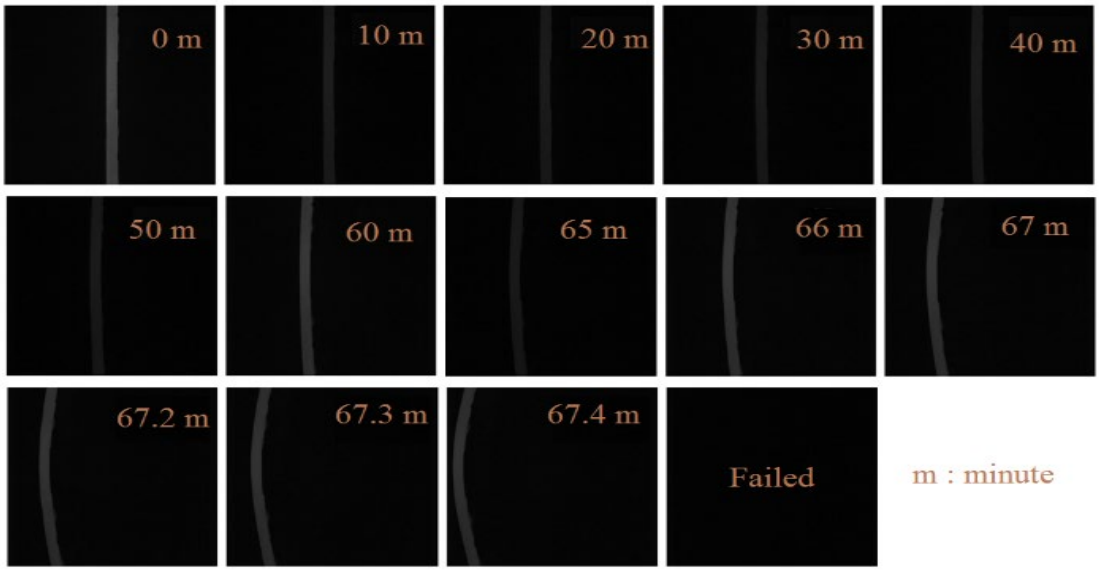

Fig. (6) Images of the test column deformation while creep buckling testing.

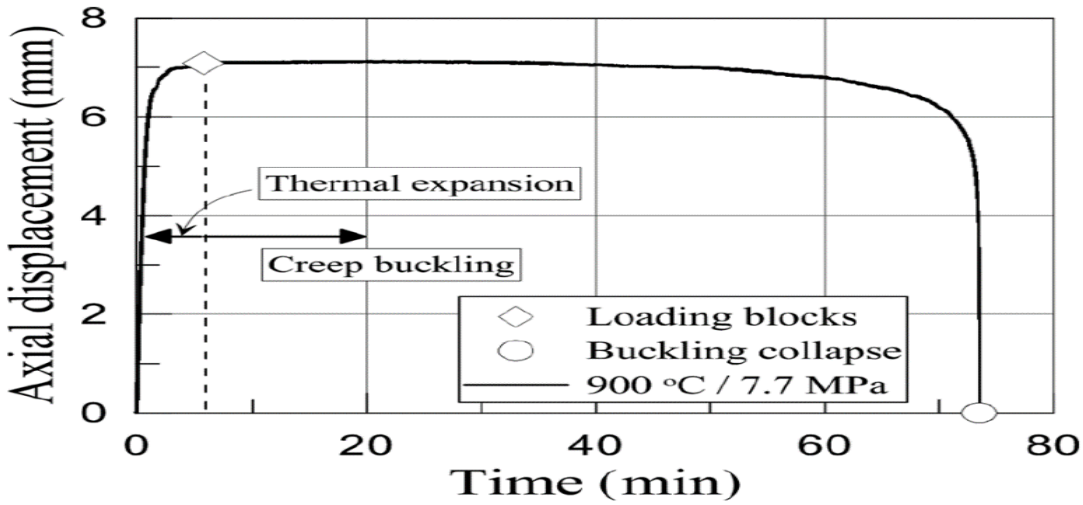

Fig. (7) Axial (in-plane) shift curve at axial compression at 900 ºC.

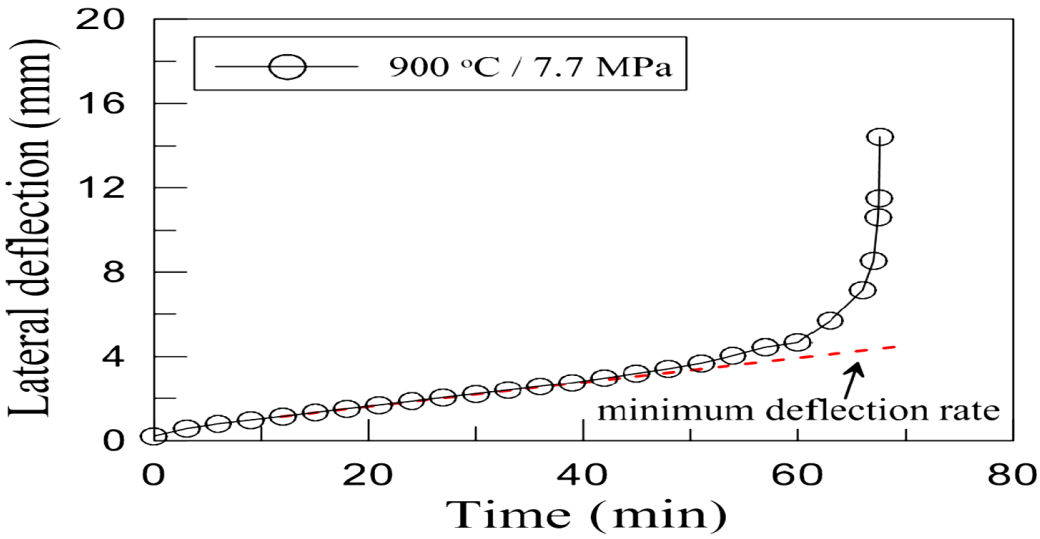

Fig. (8) Lateral (out-of-plane) deflection curve at a compression of 900 °C.

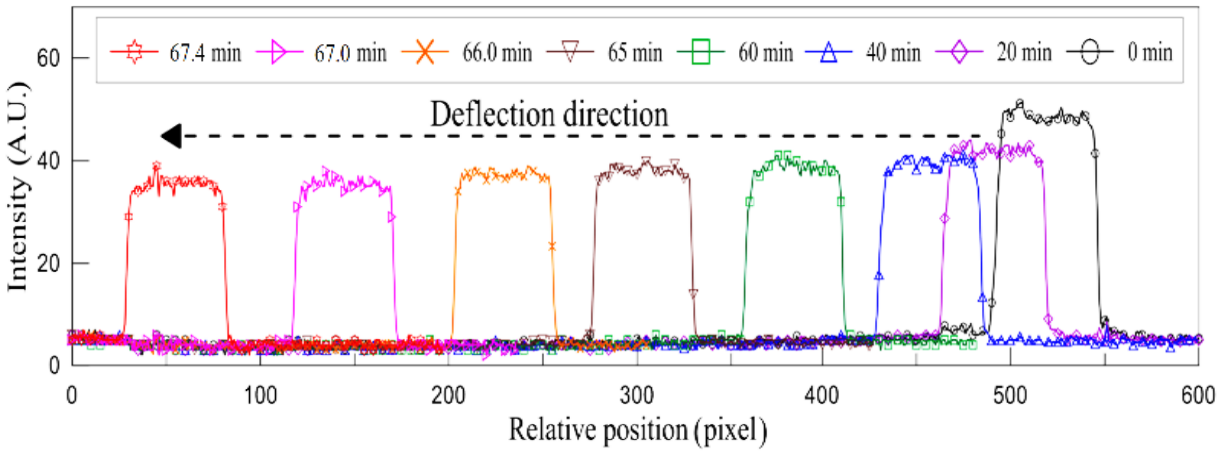

Fig. (9) Images intensity plots of the test column in the test of buckling.

Creep Buckling

Fig. 9 is the creep buckling the plate column failure times beneath axial compression at 800, 900, and 1000 °C. Fig. 9(a) is the linear axes. Then, the time to failure (crumble) multiplied significantly reducing compressive stress. At 800 °C. These stresses ranged from 95 % to 80 % of the stress to the columns and the failure instances was different 3.1 and 186 min. At 900 °C, the stresses ranged from 39% to 80% of the stress were conducted, and we determined the plate column failure between 1.1 and 198 min. At 1000 °C, the buckling failure ranged 0.4 and 118 min at stresses of 15–80% at the same temperature. The influences of the experiments indicate that better temperatures can add critical impact on the creep failure time at 800 and 900 °C well-known indicating a buckling collapse before the latter temperature with a lower stress ratio to buckling strain. This comparative function shifted greater outstanding for a thousand °C. Here, the test column collapse is by buckling for less than 120 minutes. below a compressive stress of most effective 15% of the buckling strain. “The slopes in Fig. 9(b) plotted on logarithmic axes are proportioned with temperature. This is a rise in the test temperature reducing the falling apart time of the chrome stainless steel column at axial compression. This happened due to the exchange within the modulus of elasticity (young’s modulus) of SUS304 with temperature. The elasticity of SUS304 modulus is not linearly proportioned to the temperature” [1,12–14], in particular decreasing a greater swiftly with growing temperature above 800 °C. Jo et al. [10] stated that the sharp decline of the younger’s modulus at temperatures above 800 °C was responsible for a drastic decrease of the buckling load under axial compression. For that reason, the decreased elastic modulus reduced he stiffness of the test column and as a result the failure time rising temperature. The scarcity of statistics of experiments on the buckling of SUS304 plate columns at very excessive temperatures had made the verification of the experimental findings difficult of a look

at with in terms of comparison. Yet, the determined tendencies of the creep buckling failure time under axial compressive stress are similar to the previously observed.

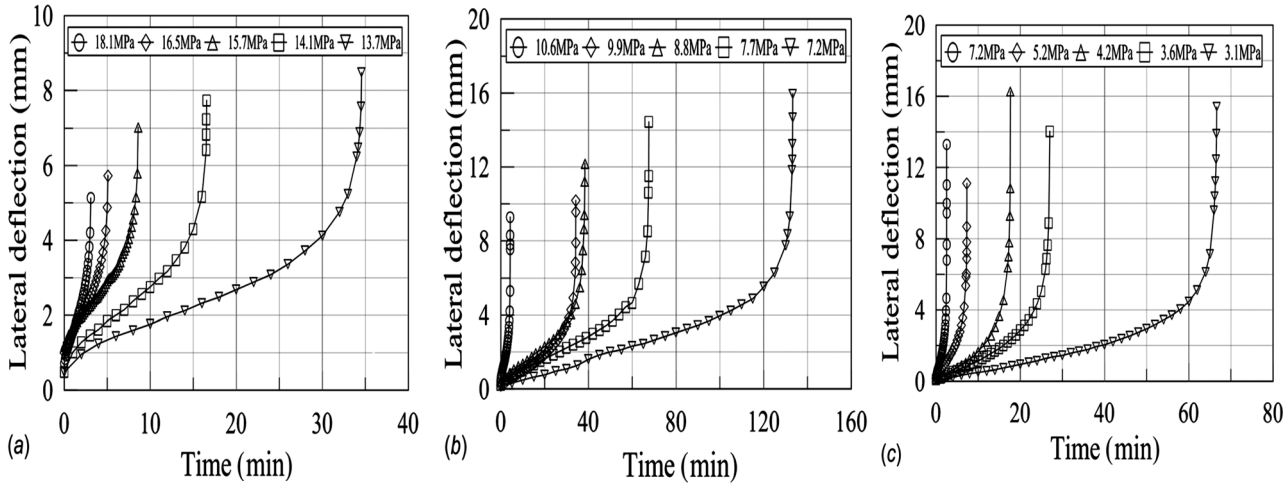

Fig. (10) Lateral deflection curve in opposition to time (a) 700 ºC, (b) 800 ºC, and (c) 900 ºC

Mechanical results

Table (1) Mechanical Test of normal-temperature specimens.

Specimen grade	$\boldsymbol{E_0/(N/mm^2)}$	$\boldsymbol{\sigma_{0.2}/(N/mm^2)}$
Steel 1312	185,885	251.3
$\boldsymbol{\sigma_u/(N/mm^2)}$	$\boldsymbol{\varepsilon_{0.2}}$	$\boldsymbol{\varepsilon_u}$
702.1	0.0029	0.5

where: E_0 is the elastic modulus; $\sigma_{0.2}$ refers to nominal yield stress, that corresponds to a residual deformation of 0.2%; σ_u stands for the final stress and $\varepsilon_{0.2}$ is the strain that correspond to $\sigma_{0.2}$; ε_u is the last stain.

Table (2) Steady-state test specimen dimensions of at high temperatures is measured.

Specimen thickness t (mm)	**Specimen width b (mm)**	**Specimen elevated temp.**
4.02	15.05	700
3.99	15.14	800
3.96	15.2	900
Elongation $\boldsymbol{\delta_{u,\theta}}$	**Final gauge length L_f (mm)**	**Initial gauge length L_0 (mm)**
0.66	83.44	50
1.2	110.3	50
1.26	119.4	50

Table (3) Mechanical test results of the high-temperature specimens.

Specimen elevated temp. ºC	$\boldsymbol{E_0/(N/mm^2)}$	$\boldsymbol{\sigma_{0.2}/(N/mm^2)}$
700	133,3	112.9
800	101,211	81.7
900	84.81	62.32
$\boldsymbol{\sigma_u/(N/mm^2)}$	$\boldsymbol{\varepsilon_{0.2}}$	$\boldsymbol{\varepsilon_u}$
253.1	0.0027	0.25
151.1	0.011	0.2
120.61	0.015	0.17

Table (4) High-temperature features decrease factors of 1312 steel.

Temperature (˚C)	$k_{cu} = \varepsilon_{u,\theta}/\varepsilon_{u0}$	$k_{\sigma u} = \sigma_{u,\theta}/\sigma_{u,0}$
700	0.5	0.36
800	0.4	0.215
900	0.34	0.171
$k_{\sigma 0.2} = \sigma_{0.2,\,A}/\sigma_{0.2,0}$		$k_E = E_\theta/E_0$
0.717		0.5
0.544		0.325
0.456		0.248

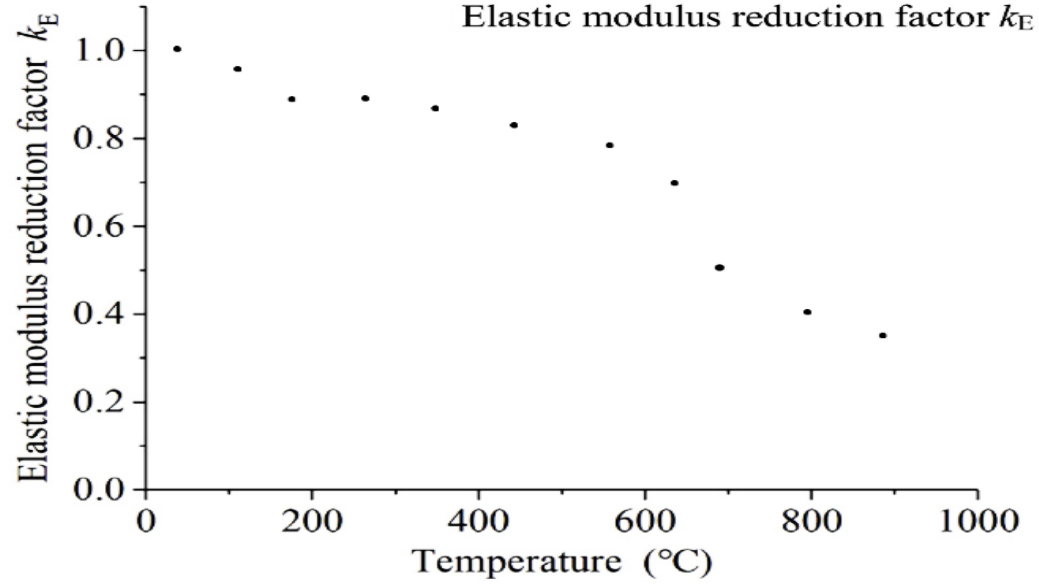

Fig. (11) Elastic modulus reduction factor k_E for 1312 elevated temp.

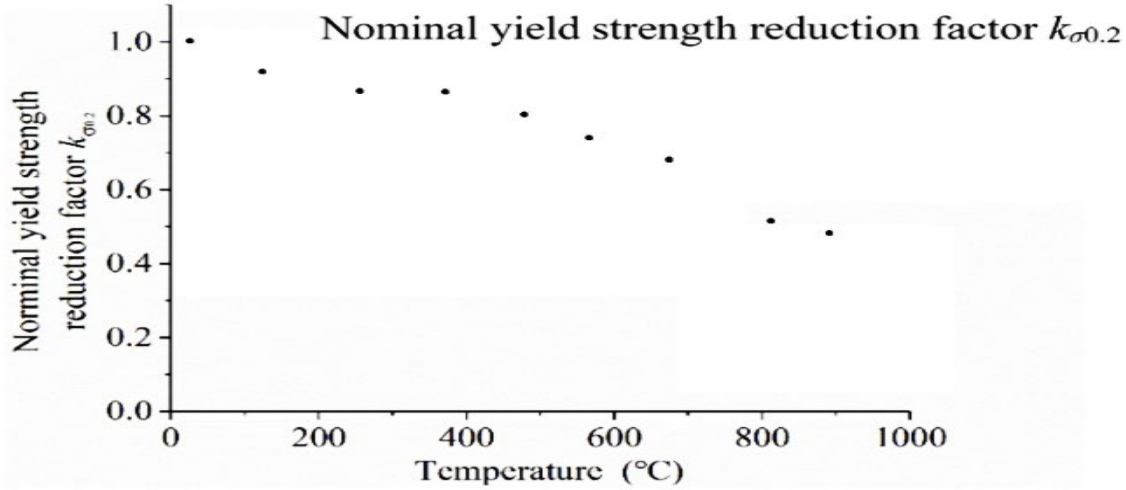

Fig. (12) Normal yield strength reduction factor $k\boldsymbol{\sigma_{0.2,}}$ for 1312 elevated temp.

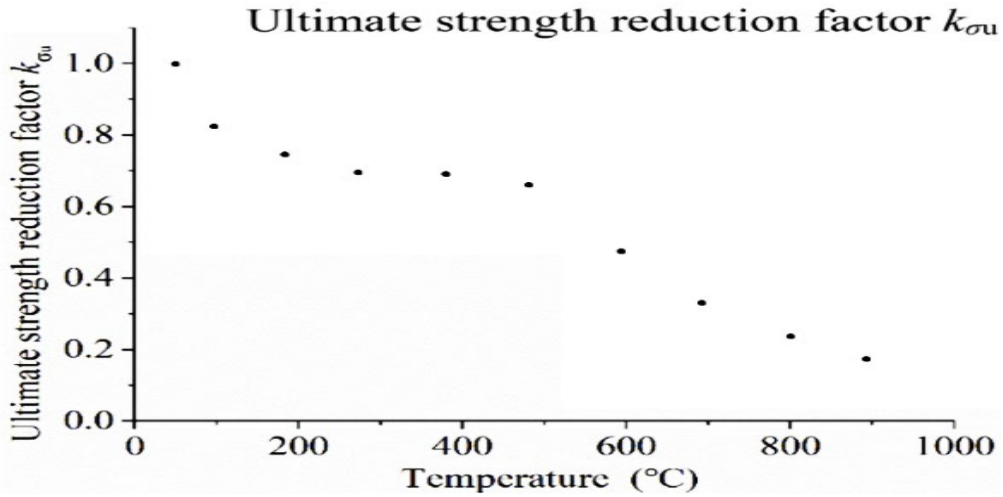

Fig. (13) Ultimate strength reduction factor k$\boldsymbol{\sigma_u}$, for 1312 elevated temp.

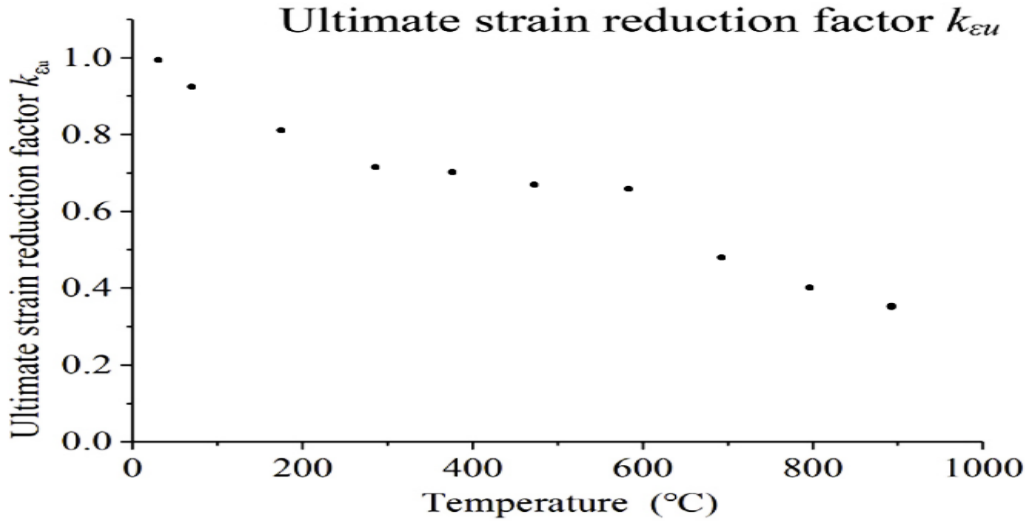

Fig. (14) Ultimate strain reduction factor k$\boldsymbol{\varepsilon_u}$, for 1312 elevated temp.

4. Conclusion

Creep buckling test was conducted. The tests are at axial compression on a Type-1312 steel plate column at 700, 800, and 900 ºC which are very high. Buckling collapse occurred in short periods (less than one and half hours even when there a load of 25% of the buckling at 900 ºC) in comparison with the creep failure at tensile stress. Here, the temperatures impacted this buckling more critically when they are high. Thus, the effect of temperature on in the stress at a is confirmed. This shows there is a positive correlation between the slope failure times in opposition to this curve to temperature. The plate column buckling collapse was depicted, in lateral deflection for developing a different empirical correlation according to the minimum rates of deflection:

a) There is a negative correlation between the test temperature and creep buckling failure time. Also, steel plate Buckling collapse happened rapidly with the increase in temperatures under the same buckling stress of each temperature.

b) The mechanical features including the in (axial) and out-of-plane (lateral) deflections showed how the plate column deforms when creep buckling happened while there was an axial compression. This happens both the in-plane and out-of-plane displacements with the quick collapse of the plate column with failure time.

c) The reductions in Elastic modulus, Normal yield strength, Ultimate strain and Ultimate strength are semi proportional with low deviation as temp. became higher.

d) Yield strain behave as tick mark between decreasing for 700 ºC and increasing for (800, 900) ºC respectively because of the hysterias loops effects.

References

[1] John A. Purkiss and Long-yuan Li, Fire Safety Engineering Design of Structures, CRC Press Taylor &. Francis, (2014).

[2] Byeongnam Jo, Koji Okamoto, Experimental Investigation into Creep Buckling of a Stainless-Steel Plate Column Under Axial Compression at Extremely High Temperatures, Journal of Pressure Vessel Technology, FEBRUARY (2017), Vol. 139.

[3] Kankanamge, D. and Mahendran, M. Behaviour and design of cold-formed steel beams subject to lateral-torsional buckling at elevated temperatures. Thin-Walled Structures, (2012) 61, 213–228.

[4] Kirby, B.R., Lapwood, D.J. and Thompson G. The Reinstatement of Fire Damaged Steel and Iron Framed Structures. Rotherham: Swinden Technology Centre, (1986).

[5] Latham, D.J., Kirby, B.R. and Thompson G. The temperatures attained by unprotected structural steelwork in experimental natural fires. Fire Safety Journal, (1987) 12, 139–152.

[6] Liew, J. and Chen, H. Explosion and fire analysis of steel frames using fiber element approach. Journal of Structural Engineering, (2004) 130, 991–1000.

[7] Lua, H., Zhao, X.L. and Han, L.H. Fire behaviour of high strength self-consolidating concrete filled steel tubular stub columns. Journal of Constructional Steel Research, (2011) 65, 1995–2010.

[8] Nadjai, A., Bailey, C.G., Vassart, O. et al. Full-scale fire test on a composite floor slab incorporating long span cellular steel beams. The Structural Engineer, (2011) 89, 18–25.

[9] Mossa, P.J., Dhakal, R.P., Bong, M.W. et al. Design of steel portal frame buildings for fire safety. Journal of Constructional Steel Research, (2009) 65, 1216–1224.

[10] Ranawaka, T. and Mahendran, M. Experimental study of the mechanical properties of light gauge cold-formed steels at elevated temperatures. Fire Safety Journal, (2009) 44, 219–229.

[11] Shahbazian, A. and Wang, Y., Direct strength method for calculating distortional buckling capacity of cold-formed thin-walled steel columns with uniform and non-uniform elevated temperatures. Thin-Walled Structures, (2012) 53, 188–199.

[12] Meijing Liu, Shenggang Fan, Runmin Ding, Guoqiang Chen, Erfeng Du, Kun Wang, Experimental investigation on the fire resistance of restrained stainless-steel H-section columns, Journal of Constructional Steel Research 163 (2019) 105770.

[13] Y. Li, W.G. Li, X.H. Zhang, et al., Modeling of temperature dependent yield strength for stainless steel considering nonlinear behaviour and the effect of phase transition, Constr. Build. Mater. 159 (2018) 147e154.

[14] Fahem, A.H., Fareed, M.M., Kadhum, M.M., Lafta, O.A., The Effect of Cyclic Twist Angle on Mechanical Properties for AISI 1038 Medium Carbon Steel, Periodicals of Engineering and Natural Sciences this, (2021), 9(3), pp. 98–105

[15] Jo, B., Sagawa, W., and Okamoto, K., "Buckling Behaviors of Metallic Columns Under Compressive Load at Extremely High Temperatures," ASME Paper, (2014) No. PVP2014-28683.

[16] Jo, B., Sagawa, W., and Okamoto, K., "Measurement of Buckling Load for Metallic Plate Columns in Severe Accident Conditions," Nucl. Eng. Des., (2014) 274, pp. 118–128.

[17] Frano, R., and Forasassi, G., "Experimental Evidence of Imperfection Influence on the Buckling of Thin Cylindrical Shell Under Uniform External Pressure," Nucl. Eng. Des., (2009) 239(2), pp. 193–200.

[18] Turner, A. P. L., and Martin, T. J., “Cyclic Creep of Type 304 Stainless Steel During Unbalanced Tension-Compression Loading at Elevated Temperature,” Metall. Trans. A, (1980) 11(3), pp. 475–481.

[19] Furumura, F., Ave, T., and Kim, W. J., “Creep Buckling of Steel Columns at High Temperatures—Part II: Creep Buckling Tests and Numerical Analysis,” J. Struct. Constr. Eng., (1986), 361, pp. 142–151.

[20] Zeng, J. L., Tan, K. H., and Huang, Z. F, “Primary Creep Buckling of Steel Columns in Fire,” J. Constr. Steel Res., (2003), 59(8), pp. 951–970.

[21] Hawas, M.N., Fahem, A.H., Design of Steam Turbine Blade Under Centrifugal Force Effect with Mutation of Rotational Speed and Blade Tongue Length, International Journal of Mechanical Engineering, (2022), 7(1), pp. 649–656.